J. Biochem. 122, 1092-1104 (1997)

Crystal Structure of 3-Isopropylmalate Dehydrogenase from the Moderate Facultative Thermophile, *Bacillus coagulans*: Two Strategies for Thermostabilization of Protein Structures[1]

Daisuke Tsuchiya,* Takeshi Sekiguchi,† and Akio Takenaka*,[2]

*Department of Life Science, Faculty of Bioscience and Biotechnology, Tokyo Institute of Technology, Midori-ku, Yokohama 226; and †Department of Fundamental Science, Faculty of Science and Technology, Iwaki Meisei University, Fukushima 970

Received for publication, May 28, 1997

The crystal structure of 3-isopropylmalate dehydrogenase from the moderate facultative thermophile *Bacillus coagulans* (BcIPMDH) has been determined by the X-ray method. BcIPMDH is a dimeric enzyme composed of two identical subunits, each of which takes an open α/β structure with 11 α-helices and 14 β-strands. The polypeptide is folded into two domains. The first domain is composed of residues 1-101 and 257-356, and the second domain, of residues 102-256. The latter domains of the two subunits are associated with one another by a dyad axis to make the dimer, locally forming a β-sheet and a four-helix bundle. As compared with the structure of the enzyme from the extreme thermophile *Thermus thermophilus* (TtIPMDH), a new short β-sheet (residues 329-330 and 340-341) absent in TtIPMDH is formed by the insertion of 5 residues in BcIPMDH. In terms of determinants for thermostabilization, both consistent and inconsistent changes were found between the two enzymes. The regions including inconsistent changes are formed by different usages of the determinants for stabilizing the loops at different levels. Those in BcIPMDH contain some structural redundancies in length of amino acid sequence and flexibility of residues, which seem to be unnecessary for the enzymatic reaction. Such redundancies are also found in the primary structure of the enzyme of the mesophile *Bacillus subtilis*, but these parts are more stabilized in BcIPMDH by hydrogen bonds and salt bridges. On the other hand, TtIPMDH is stabilized by reducing such redundant parts. This contrast suggests that different strategies may be preferred for thermostabilization, depending on temperature.

Key words: *Bacillus coagulans*, crystal structure, 3-isopropylmalate dehydrogenase, thermostability, X-ray analysis.

Denaturation, that is, loss of higher-order structures, interferes with protein function. To prevent this, it is essential to understand the structural basis of the stability of proteins. Thermal resistance is especially important for designing new functional proteins. Guidelines for achieving thermostabilization could not only allow the production of more stable proteins, but also extend the effective temperature range of protein functionality.

Several determinants of the thermostabilization of proteins have been proposed (*1-3*), and many trials have been performed to replace amino acids in order to stabilize proteins by design, but with limited success. Most of the proposed determinants have been deduced from structural comparisons between extremely different proteins, highly thermostable and thermolabile. However, structural knowledge of moderately thermostable proteins might give a better understanding of the kinds of structural changes that influence protein thermostability.

IPMDH [EC 1.1.1.85] is an enzyme in the leucine biosynthesis pathway (*4*). We have determined the crystal structure of IPMDH from the moderate, facultative thermophile *Bacillus coagulans* (BcIPMDH). This organism proliferates in temperatures ranging from 25 to 61°C (*5*). BcIPMDH itself is also moderately thermostable (*6*). Recently the crystal structures of EcIPMDH and StIPMDH, which are more thermostable than BcIPMDH, have been solved and compared with that of TtIPMDH (*7*). Our crystal structure of BcIPMDH will provide information about another level of thermostabilization, *i.e.*, that in the moderate thermophile, *Bacillus coagulans*. In this paper, the structural characteristics of BcIPMDH are described and compared with those of TtIPMDH, and then several determinants of thermostabilization are examined in relation to thermostability. Finally we will discuss the nature of

[1] This work was supported in part by Grants-in-Aid for Scientific Research on Priority Areas (No. 08214203, 07230224, and 07250205) from the Ministry of Education, Science, Sports and Culture of Japan, and by the Sakabe project of TARA (Tsukuba Advanced Research Alliance), University of Tsukuba, Japan.

[2] To whom correspondence should be addressed. Phone: +81-45-924-5709, Fax: +81-45-924-5748, E-mail: atakenak@bio.titech.ac.jp

Abbreviations: IPMDH, 3-isopropylmalate dehydrogenase; BcIPMDH, *Bacillus coagulans* IPMDH; TtIPMDH, *Thermus thermophilus* IPMDH; BsIPMDH, *Bacillus subtilis* IPMDH; EcIPMDH, *Escherichia coli* IPMDH; StIPMDH, *Salmonella typhimurium* IPMDH; tMDH, *Thermus flavus* malate dehydrogenase; cMDH, porcine heart malate dehydrogenase.

the strategies for thermostabilization in IPMDHs.

METHODS

Three crystalline forms of BcIPMDH were obtained by the hanging drop vapor diffusion method using ammonium sulfate or polyethylene glycol 2000 as a precipitant. The conditions are described elsewhere (*8*). The trigonal form (Table I) was used for the present analysis. X-ray diffractions of two crystals mounted with different orientations were recorded on imaging plates with a Weissenberg camera (*9*) using synchrotron radiation ($\lambda = 1.00$ Å) at the Photon Factory in Japan. Data processing and reduction were performed with the program WEIS (*10*) and the CCP4 software (*11*).

Since the trigonal form contains one dimeric molecule in the asymmetric unit, a dimeric probe molecule with all alanines was constructed from TtIPMDH (*12*) and applied to molecular replacement to solve the crystal structure. The program AMoRe (*13*) gave a unique solution with a reasonable molecular packing. Its plausibility was further confirmed by the R_{omit} profile analysis (*14*). The initial phases were improved by a density modification technique with non-crystallographic symmetry averaging between the two subunits, solvent flattening and histogram mapping using the program DM (*15*). Combinations of model-building with the program O (*16*) and refinement of the atomic parameters with the program X-PLOR (*17*) gave a final R-factor of 0.180 for the data of 10-3.0 Å resolution, with a free-R value (*18*) of 0.247 for the 10% of reflection data which were not used throughout the refinement.

The stereochemical parameters calculated with the program PROCHECK (*19*) are better than those for ordinary protein structures determined at 3.0 Å resolution. The mean B-factor is somewhat high, 38 Å^2 for main-chain atoms and 43 Å^2 for side chain atoms. This may be a consequence of the high solvent content of the crystal and partial conformational disorder which prevents the observation of X-ray data beyond 3.0 Å resolution. Electron densities on $2F_o - F_c$ and omit maps, however, showed good quality even in loop regions, as seen in Fig. 1.

TABLE I. **Crystal data and refinement statistics for BcIPMDH.**

Space group	$P3_121$
Cell constants (Å)	
$a = b$	114.4
c	194.9
Z^a	2
$V_{solv.}$ (%)	73
Limiting resolution (Å)	3.0
Observed reflections	101,970
Independent reflections[b]	25,540
R_{merge} (%)	5.4
Completeness (%)	85.3 (total)
	62.9 (3.16-3.00 Å resolution shell)
Non-hydrogen protein atoms	5,439
Solvent molecules	3
Reflections used for refinement	24,637
Resolution range (Å)	10-3.0
R-factor (%)	18.0
R_{free}[c] (%)	24.7
R.m.s. standard deviation	
Bond length (Å)	0.006
Bond angles (°)	1.30
Improper angles (°)	1.20
Average error (Å)	0.35

[a]Number of subunits in the asymmetric unit. [b]$I > 3.0\sigma$. [c]Calculated using the 10% of reflection data which were not used through refinement.

RESULTS AND DISCUSSION

Description of the Structure—BcIPMDH is a dimeric enzyme composed of two identical subunits, each of which has the molecular weight of 39,808 with 366 amino acid residues (*20*). The crystal used for the present analysis contains one dimeric enzyme in the asymmetric unit. The two subunit structures have been determined independently. We located 356 residues in subunit I and 357 residues in subunit II on electron-density maps, but 10 and 9 residues at the C-termini of the subunit I and II, respectively, were not assigned owing to their disordered structures. The two subunits can be superimposed with an r.m.s. displacement of 0.54 Å between the corresponding C_α positions. As the average error of the structure is estimated to be 0.35 Å from a Luzzati plot (*21*), the two subunits have essentially the same tertiary structure. There are only a few intermolecular contacts in the crystal, because it has a rather high solvent content of 73% (*8*). Here we will describe the structure of subunit I, because the local structures are almost the same in the two subunits and subunit I has fewer intermolecular contacts.

Each subunit takes an open α/β structure with 11 α-helices and 14 β-strands (Fig. 2). The polypeptide is folded into two domains. The first domain is composed of residues 1-101 and 257-356, and the second, of residues 102-256. The latter domains are associated with one another by a dyad axis to make the dimer, and locally to form a β-sheet and a four-helix bundle.

Structural Comparison between BcIPMDH and TtIPMDH—A sequence alignment between BcIPMDH and TtIPMDH based on their three-dimensional structures is shown in Fig. 3. The amino acid sequence of TtIPMDH has 10 gaps as compared with BcIPMDH. In addition, BcIPMDH is longer by 2 residues at the N-terminus and by 10 residues at the C-terminus. As expected, the three-dimensional structures are similar, with an r.m.s. displacement of 1.3 Å. Figure 4 indicates local differences in C_α position between BcIPMDH and TtIPMDH. The whole structures are well conserved, though some significant differences occur in loop regions. A new short β-sheet (residues 329-330 and 340-341) absent in TtIPMDH is formed by the insertion of 5 residues in BcIPMDH (Fig. 3).

Crystal structures of TtIPMDH complexed with NAD (*25*) and with the substrate (*26*) have been reported. Although the present BcIPMDH contains neither the cofactor nor the substrate, structural comparison among them will give some information about the enzymatic function.

As all residues which participate in binding to the cofactor/substrate in TtIPMDH are conserved in BcIPMDH (Fig. 3), the same binding features can be expected in BcIPMDH. Figure 5a shows the NAD binding site found in TtIPMDH (*25*), on which the unliganded BcIPMDH and TtIPMDH are superimposed. Comparison of the local structures[3] between the two unliganded structures indicates significant differences in the two loops (residues 253-262 and 327-343). In the former loop of TtIPMDH, some

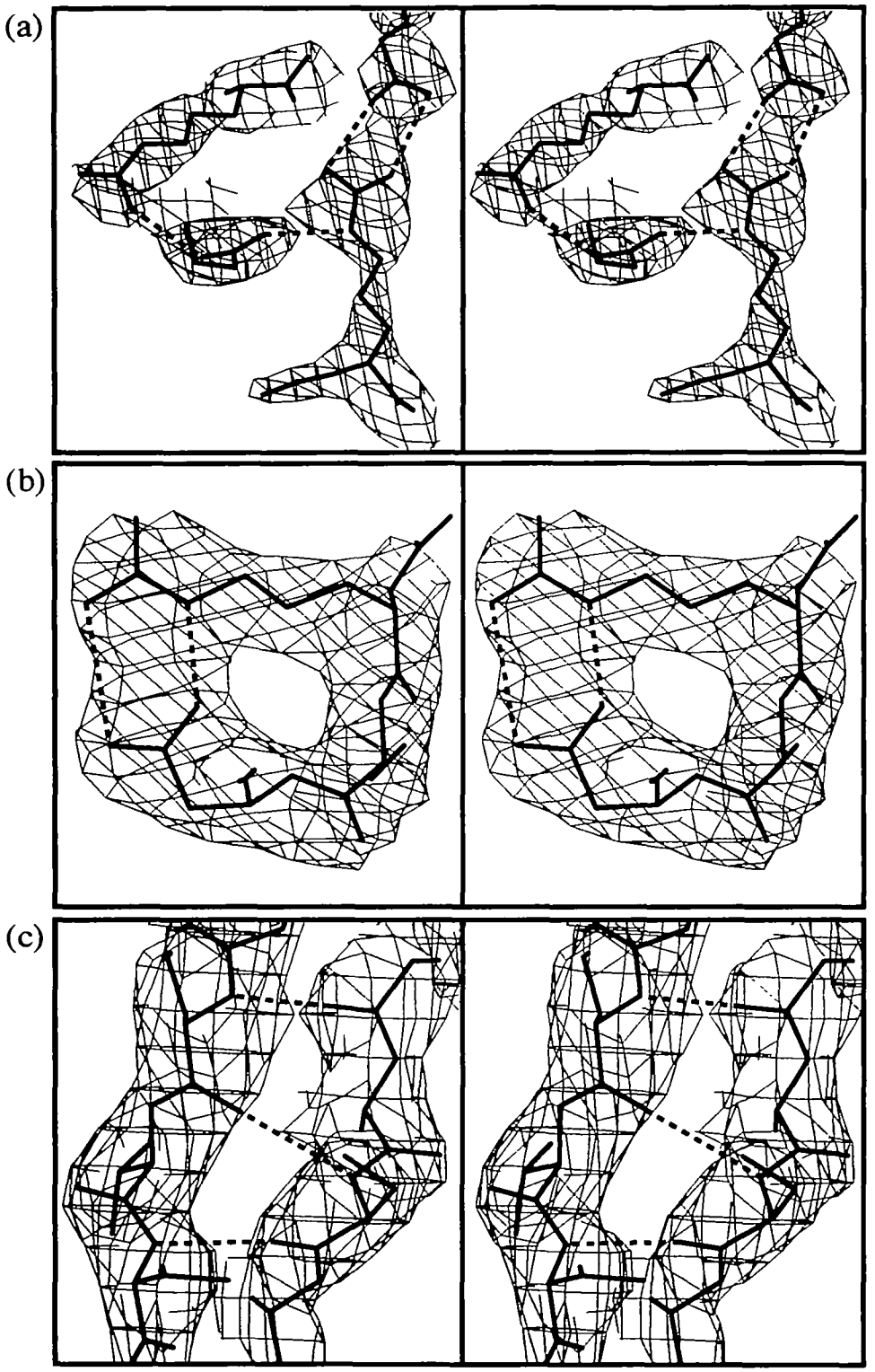

Fig. 1. **Stereo-pair diagrams of omit maps (contoured at the 2σ level) of (a) salt-bridging residues around the loop A region, (b) those around the loop B region, and (c) a new β-sheet in the loop C region.** Hydrogen bondings are indicated by broken lines. These diagrams were produced with the program O (*16*).

conformational change of the mainchain is required for the cofactor binding (*25*). In the case of BcIPMDH, the corresponding loop will move further than that of TtIPMDH, as seen in Fig. 5b. Figure 3 shows that only the replacement of the amino acid at position 256 with more flexible threonine (TtIPMDH:Pro251→BcIPMDH:Thr256) makes such movement possible in BcIPMDH. These features suggest that the loop of BcIPMDH has greater flexibility than is necessary to bind the cofactor, as discussed later. Such

[3] To compare several local structures including loops between BcIPMDH and TtIPMDH, packing effects on the conformations were examined by calculation from the atomic coordinates. It has been confirmed that the corresponding local structures in TtIPMDH are not affected significantly.

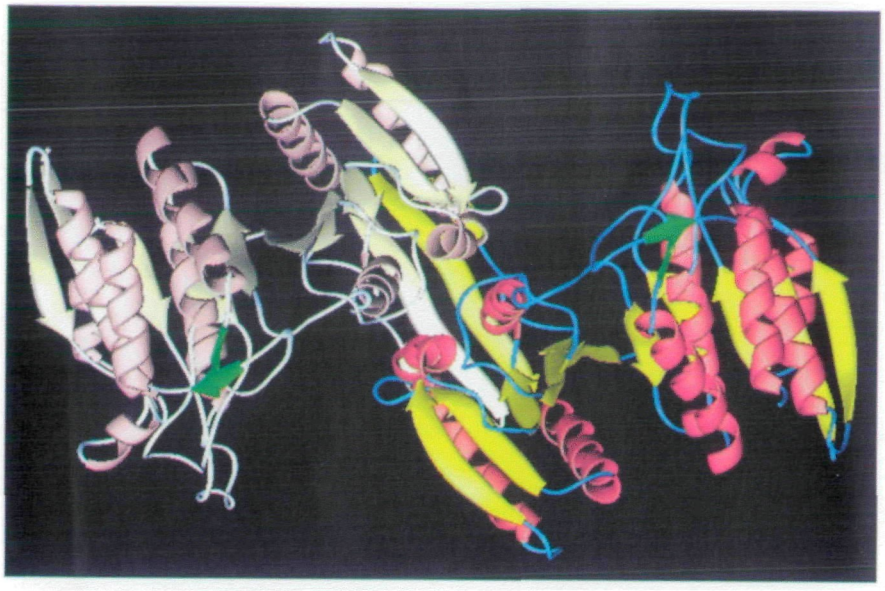

Fig. 2. **A ribbon drawing of the dimeric structure of BcIPMDH viewed down the molecular twofold axis.** The subunits I and II are represented by saturated and unsaturated colors, respectively. The new β-sheets found in BcIPMDH are colored green. This picture was produced with the program RIBBONS (*22*).

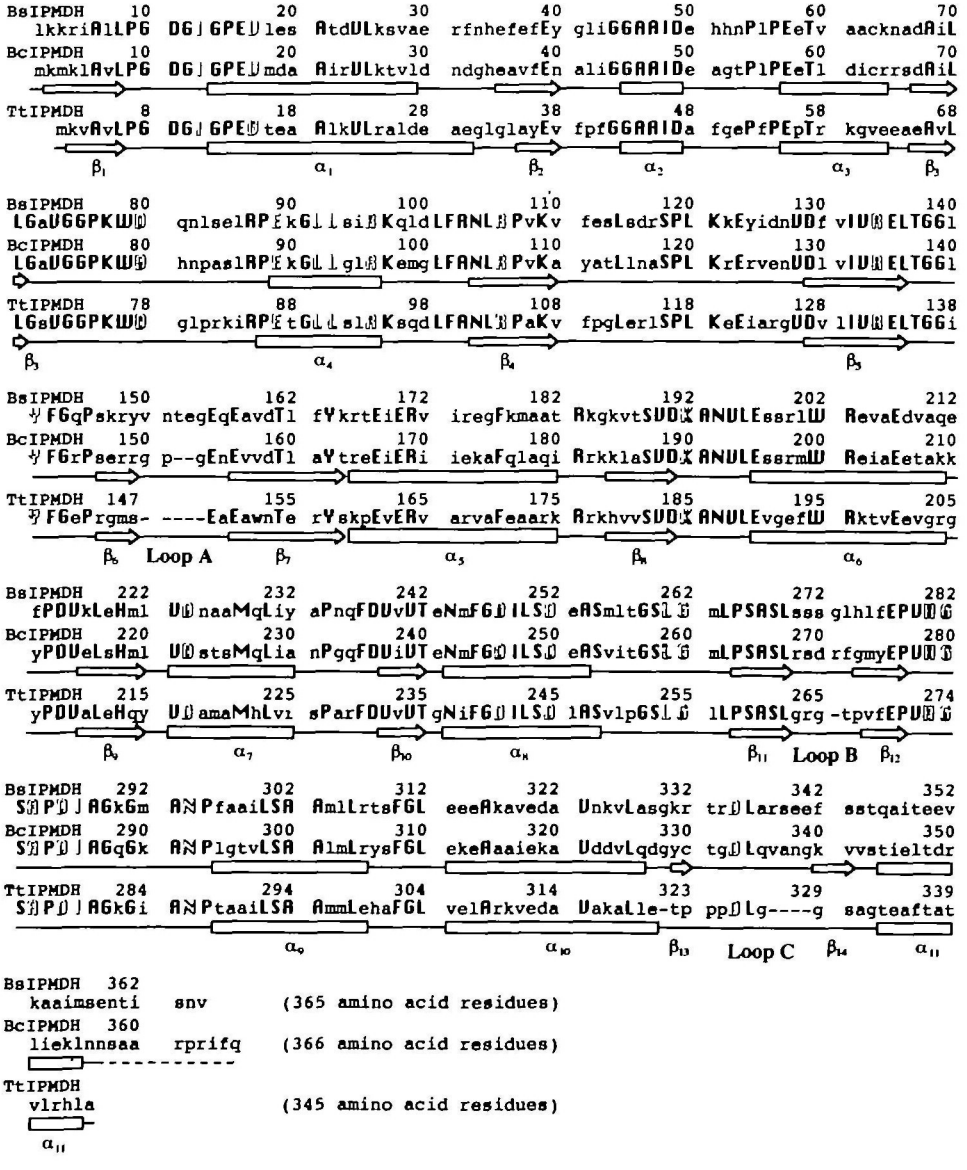

Fig. 3. **Primary and secondary structures of three IPMDHs (*12, 20, 23, 24*).** Upper-case letters, lower-case letters, and hyphens, respectively, indicate identical amino acids, different ones, and gaps. BcIPMDH has sequence identities of 60% with BsIPMDH and 51% with TtIPMDH. The identity between BsIPMDH and TtIPMDH is 54%. Residues which may contact with the substrate (*26*) and/or the cofactor (*25*) are shown with outlined letters. α-Helical and β-stranded regions are represented with rectangles and arrows, respectively. The numbering of the secondary structures is shown at the bottom.

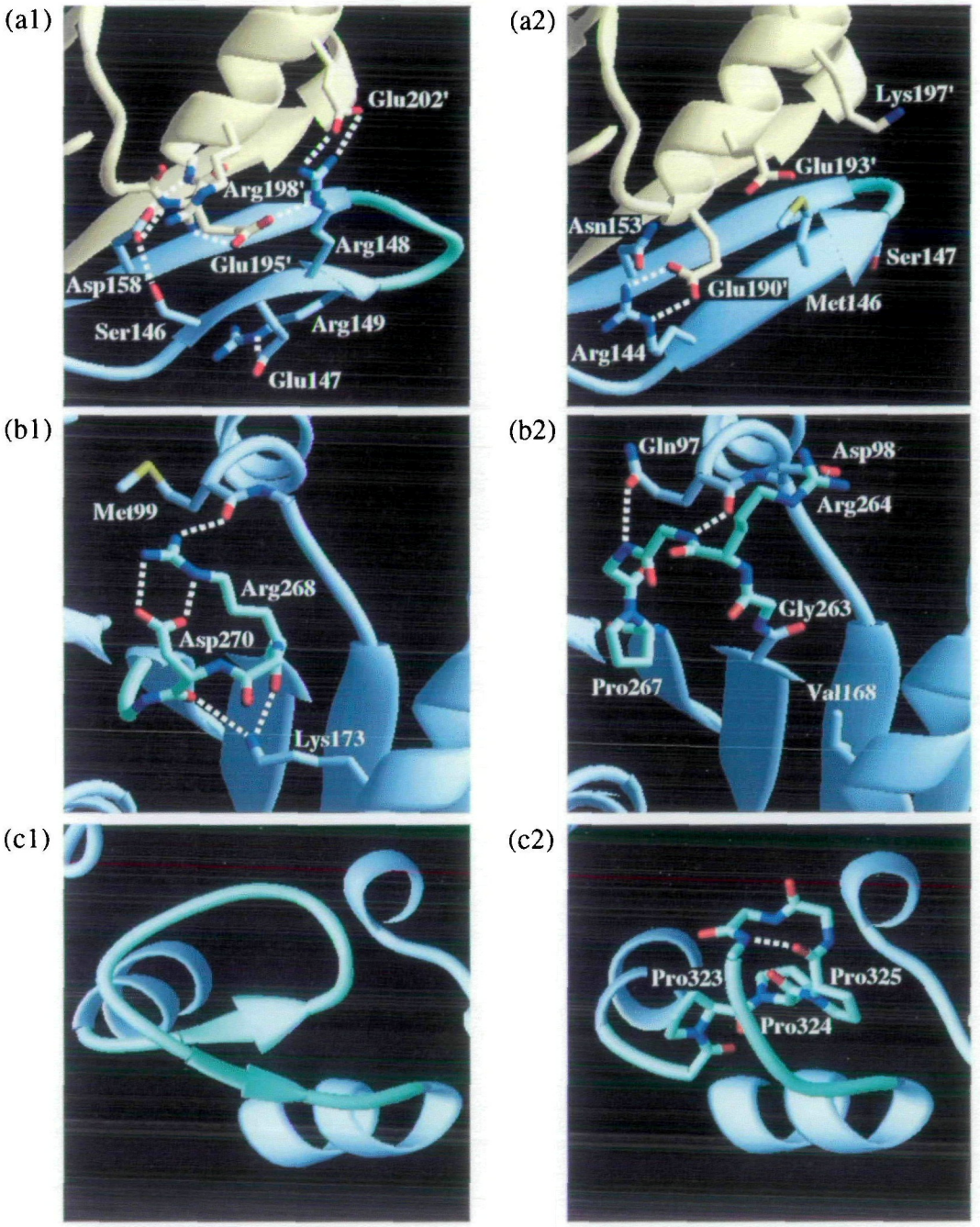

Fig. 8. **Local structures around loop A of BcIPMDH (a1) and TtIPMDH (a2), loop B of BcIPMDH (b1) and TtIPMDH (b2), and loop C of BcIPMDH (c1) and TtIPMDH (c2).** These loops and the other parts in subunit I are shown in green and blue, respectively. The two β-strands connected by loop A form a β-sheet with a strand from the other subunit (orange). Broken lines indicate possible hydrogen bonds. All the pictures were produced with the program RIBBONS (*22*).

non-Pro→Pro replacement is one of the general rules for thermostabilization of proteins (*28–30*), and is consistent with the difference in thermostability between the two enzymes. The loop region of residues 327–343 is lengthened by 5 residues in BcIPMDH to form a new short β-sheet as mentioned above (Fig. 5a). However, it should be noted that Asp333 and its neighbors which are close to the cofactor are retained among the three structures. For this reason, the large difference observed in this loop does not affect the cofactor binding. In addition, this loop contains three proline residues (Pro323, 324, and 325; see Fig. 3) in TtIPMDH.

Comparison of Determinants for Thermostabilization between BcIPMDH and TtIPMDH—In order to investigate the origin of thermostability of proteins, several determinants for their thermostabilization have been proposed. We discuss below which determinants can well explain the difference in thermostability between BcIPMDH and TtIPMDH.

Replacement with preferred amino acid: It is reasonable

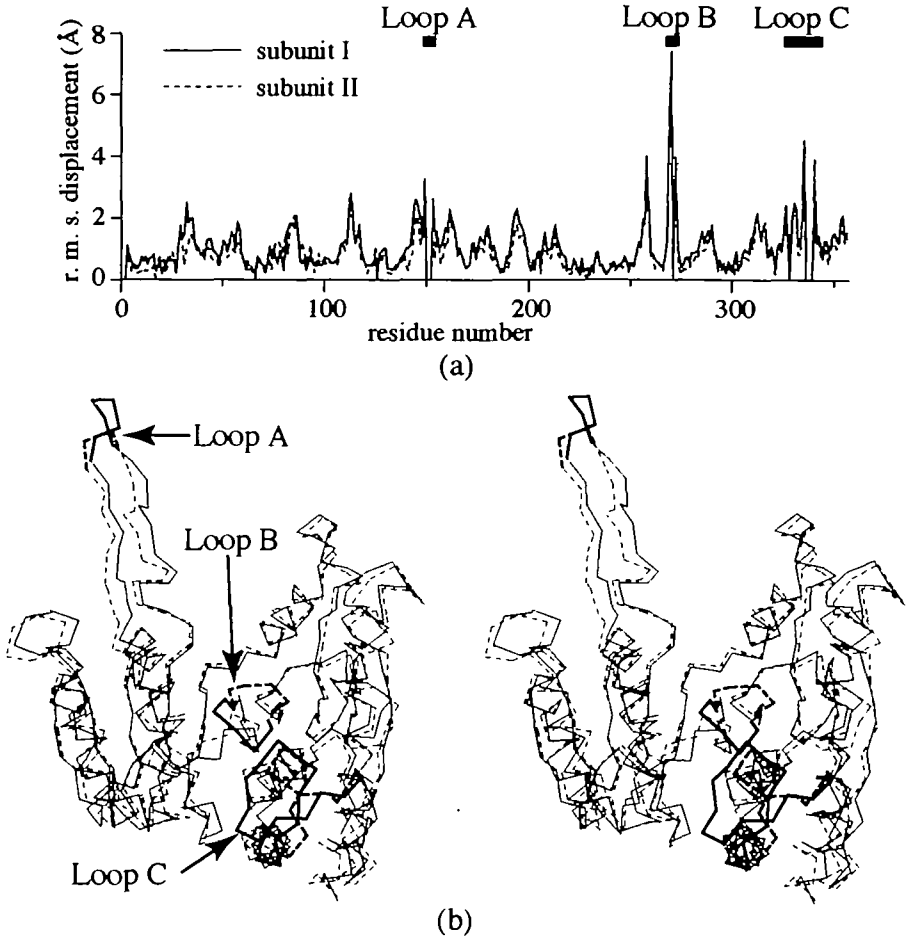

Fig. 4. **Comparison of tertiary structures between BcIPMDH and TtIPMDH.** (a) R.m.s. displacements of C_α atoms of each subunit (solid line for subunit I and broken line for subunit II) from TtIPMDH, calculated by least-squares fitting. Zero values indicate deletions of amino acid residues in TtIPMDH. (b) A stereo-pair diagram of the C_α structures superimposed between BcIPMDH (solid line for subunit I) and TtIPMDH (broken line).

to consider that thermophilic proteins contain more amino acids with properties that inhibit thermal denaturation than do the mesophilic ones. By comparing amino acid types between mesophilic and thermophilic proteins, Argos *et al.* (*31*) found several preferred substitutions of amino acids in thermophilic proteins. A series of mutants of T4 lysozyme showed that non-Pro→Pro and Gly→non-Gly exchanges contribute to the thermostability of proteins, affording a reduction in entropy of the unfolded state (*28*). Such a contribution to thermostability was also found in the other proteins (*29, 30*). Ishikawa *et al.* suggested that replacement of Gly by a residue which is forced to have a left-handed-helical conformation releases steric hindrance of the C_β atom and enhances thermostability (*32*). Amaki *et al.* demonstrated that replacement of free cysteine residues can improve thermostability (*33*).

Figure 6 shows the frequency of amino acid exchanges between BcIPMDH and TtIPMDH. The most frequent exchange is Asp→Glu in the BcIPMDH→TtIPMDH direction. This exchange agrees with the rule of Argos *et al.* (*31*). Ala→Arg and Ile→Val exchanges are also frequently observed, but the latter is reversed in direction from the preferred exchange (Val→Ile). Although the latter exchanges seem to be inconsistent, no large differences occur in hydrophobic interactions, because they are compensated by the surrounding amino acids.

Another striking difference in relation to thermostability is the number of proline residues (18 in BcIPMDH and 25 in TtIPMDH). The increase of proline residue stabilizes the protein by reducing the entropy of the unfolded state. This situation is also found in EcIPMDH and StIPMDH (*7*). The number of glycine residues increases from 31 in BcIPMDH to 36 in TtIPMDH. Although such an increase in general raises the entropy, glycine is sometimes effective to release torsional strain in loop regions (*32*). However, TtIPMDH still contains some strains. The number of non-glycines with main-chain torsion angle of $\phi > 0$ is 3 in BcIPMDH and 4 in TtIPMDH. Therefore, increasing number of prolines in TtIPMDH is consistent with higher thermostability, but increasing the number of glycines seems to be inconsistent with it.

BcIPMDH has two cysteine residues, which are replaced with other amino acids in TtIPMDH. Such exchanges may lead to thermostabilization of TtIPMDH, as demonstrated by Amaki *et al.* (*33*). Site-directed mutagenesis of the two cysteines (Cys61 and Cys330) to serines, however, caused no significant change of thermostability (Sekiguchi, unpublished data).

Ion-pairs and hydrogen bonds: Ion-pairs and hydrogen bonds have high enthalpic effects on protein folding. Perutz pointed out that introduction of a few salt bridges is effective in protecting proteins from denaturation by heat (*34*). Ion-pairs and/or hydrogen bonds play major roles in thermostabilization of indole-3-glycerol phosphate synthase from *Sulfolobus solfataricus* (*35*), glutamate dehydrogenase from *Pyrococcus furiosus* (*36*), and malate

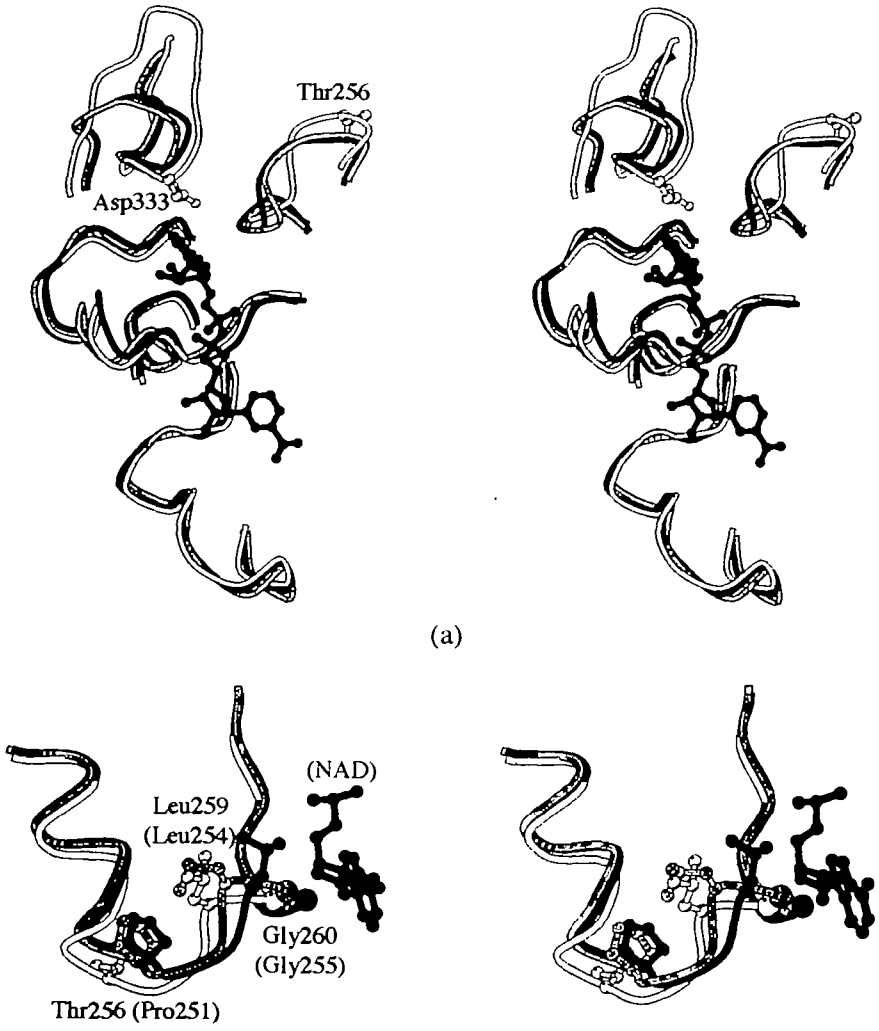

Fig. 5. **(a) A stereo-pair diagram of the NAD binding site found in TtIPMDH (dark line) (25), on which the unliganded BcIPMDH (open line; the present work) and TtIPMDH (shaded lines) (12) are superimposed.** Two loops containing Asp333 and Thr256 are discussed in the text. **(b) Difference of the local structure around Thr256.** The unliganded TtIPMDH and its NAD complex are superimposed on BcIPMDH. The corresponding residues in TtIPMDH are indicated in parentheses. The adenosine moiety of NAD is drawn. These diagrams were produced with the program MOLSCRIPT (27).

Bc \ Tt	G	A	L	I	V	P	F	M	D	E	K	R	N	Q	C	S	T	Y	H	W
G	21	2				2			1							1				
A	1	19	2		3	1	2				1	4				1				
L		1	25	2	4	1	2	1	1	2		1					1	1		
I	1	1	3	5	6		1			1	1						1			
V		6	2	1	15											1				1
P						16														
F							6										1	1		
M			1	1	1		1	3						2			1			
D	1	2							12	5	2		1							
E	3	3	2		1	2				15	1	3				1				
K	2			1	1				1	1	7	2					1		2	
R	1			1				1		6	2	8				1	1			
N	1	3	1		1							1	4			1				
Q	1		1							1	1	2							1	
C					1	1														
S	2	4			1					1	1	2				9				
T	1	2			1	2		1		1						1	6			
Y							2										1	3	1	
H	1		1																2	
W																				2

Fig. 6. **Frequency of amino acid exchanges between BcIPMDH and TtIPMDH.** Residues with no corresponding counterparts were neglected in the counting.

dehydrogenase from *Thermus flavus* (37). Tanner *et al.* suggested that hydrogen bonding between a charged side chain and a neutral partner is correlated with thermostability among four different D-glyceraldehyde-3-phosphate dehydrogenases (38).

The numbers of ion-pairs counted with three different distance criteria are listed in Table II. The buried ion-pairs with residue accessibility (39) less than 0.2 were discriminated on the basis of different effects in the interior (1). Although the difference in number of buried ion-pairs is not clear, the total number of ion-pairs in TtIPMDH is more than that of BcIPMDH, in accordance with their thermostabilities. TtIPMDH contains more solvent-exposed ion-pairs than BcIPMDH. However, according to Dao-pin *et al.* (40), such ion-pairs have little effect on thermostability. Therefore, it is difficult to rationalize the relative thermostabilities in terms of the number of ion-pairs alone.

Hydrogen bonds were assigned according to the criteria defined by Baker and Hubbard (41). Table III shows the number of hydrogen bonds (hydrogen bonds through water molecules are neglected). The buried hydrogen bonds were also discriminated with the same residue accessibility as for the buried ion-pairs. The numbers of buried hydrogen bonds are almost the same in BcIPMDH and TtIPMDH, but

TABLE II. **Number of ion-pairs counted with several cutoff distances.**

Cutoff distance (Å)	Total ion-pairs		Buried[a] ion-pairs	
	BcIPMDH	TtIPMDH	BcIPMDH	TtIPMDH
3.0	21	32	5	4
4.0	57	68	12	9
5.0	76	88	14	15

[a]Residue accessibility less than 0.2.

TABLE III. **Number of hydrogen bonds.**[a]

	BcIPMDH	TtIPMDH
Total hydrogen bonds	662	614
Buried[b] hydrogen bonds	305	311
Hydrogen bonds between		
Polar atoms	542	502
Polar and charged atoms	83	78
Charged atoms	37	34

[a]Hydrogens attached to the polar atoms were generated with the QUANTA/CHARMm program system (Molecular Simulations). [b]Residue accessibility less than 0.2.

solvent-exposed hydrogen bonds are increased in BcIPMDH. In any count of hydrogen bonds by atomic charge (Table III) BcIPMDH has a greater number than TtIPMDH. Although Tanner *et al.* pointed out a preference of hydrogen bonds between polar and charged atoms for thermostabilization (*38*), this is reversed between the two IPMDHs.

Stabilization of secondary structure: BcIPMDH is composed of 11 α-helices and 14 β-strands per subunit (Fig. 3), each of which should be stabilized to maximize overall stabilization. These secondary structures can be stabilized with hydrogen bonding at the ends by so-called capping (*3, 42*) and with electrostatic interaction between the helix dipole and a charged atom (*43*). Residues with β-branched side-chains (Val, Ile, and Thr) or glycine residues destabilize a helix when they are in an internal position (*44, 45*). Prolines at the second sites of β-turns and at the N-termini of α-helices contribute to thermostabilization in oligo-1,6-glucosidase (*30*).

Capping of the termini of helices is found in both BcIPMDH and TtIPMDH. Residues participating in capping, Ser343 for the N-terminus of helix α_{11} and Arg124 for the C-terminus of helix α_7 of BcIPMDH are, however, absent in TtIPMDH. In terms of helix capping, BcIPMDH seems to be more stabilized than TtIPMDH. On the other hand, helices in EcIPMDH and StIPMDH are less capped than in TtIPMDH (*7*).

The numbers of residues with β-branched side-chains at a helix-internal position are the same in BcIPMDH and TtIPMDH. Each enzyme contains one glycine at the helix internal position. There are no significant differences in helix-internal stabilization between the two enzymes.

As mentioned above, TtIPMDH has 7 more proline residues than BcIPMDH. Two of them are located at the N-termini of α-helices, participating in their stabilization. Other prolines except the three contiguous ones (residues 323, 324, and 325 in TtIPMDH) are found near the termini of secondary structures. TtIPMDH is thus stabilized by introducing prolines, unlike BcIPMDH which preferentially employs electrostatic capping of helices as a thermostabilization strategy.

Molecular surface and interior: In general, many hydrophobic residues are packed inside the protein to form a hydrophobic core, whereas hydrophilic residues tend to be located outside. Replacement of hydrophobic residues in the core with hydrophilic ones leads to thermal destabilization (*46*). Buried polar atoms with no hydrogen-bonding partner will make the protein unstable (*47*). Increase of cavities in proteins is a measure of such destabilization (*48*).

There is no significant difference between the numbers of completely buried polar atoms without hydrogen-bonding partners (187 atoms in BcIPMDH, and 186 atoms in TtIPMDH). On the other hand, there are more charged atoms with no partners in BcIPMDH (13 atoms) than in TtIPMDH (8 atoms). This increase is localized at the subunit interface (Fig. 7). The four-helix bundle of TtIPMDH is formed mainly by hydrophobic interaction. Leu246 in TtIPMDH is replaced with a charged residue (Glu251) in BcIPMDH. In addition, Ala220 in TtIPMDH is replaced with a polar Ser225. These differences are clearly correlated with the difference in thermostability between the two enzymes, as pointed out on the basis of site-directed mutagenesis studies (*49*) and X-ray analyses of TtIPMDH (*12*) and EcIPMDH (*7*).

Total volumes of cavities were calculated by using the program VOIDOO (*50*). The values, 4.4×10^2 Å^3 in BcIPMDH and 7.1×10^2 Å^3 in TtIPMDH, indicate that TtIPMDH contains more vacant space. In the largest cavity, Gly235 in TtIPMDH is replaced with Glu241 in BcIPMDH to fill the space and to form a capped structure at the N-terminus of helix α_8 through a hydrogen bond. This difference is not consistent with the difference in thermostability. A similar inconsistent cavity change was found in a comparison between TtIPMDH and EcIPMDH/StIPMDH (*7*).

Another determinant proposed by Chan *et al.* (*51*) is the ratio of molecular surface to enclosed volume. Although the ratio was calculated for the two IPMDH's according to Tanner *et al.* (*38*), there was no significant difference.

Two Strategies for Thermostabilization—The possible determinants of the difference in thermostability between BcIPMDH and TtIPMDH are summarized in Table IV. Among them, introduction of prolines in TtIPMDH and stabilization of its hydrophobic core are likely to be largely responsible for the extreme thermostabilization. However, several determinants seem to show inconsistent changes, as described above. It is important to note that BcIPMDH is produced in the moderate thermophile, *Bacillus coagulans*. Since organisms utilize suitable determinants to adapt their proteins to different temperatures, it is necessary to consider the preferences for determinants and their usage, *i.e.*, how they are combined and where they are introduced. Based on this idea, we have thoroughly examined the regions including these inconsistent changes in detail, and found three characteristic regions including loop structures, loop A with residues 150-154, loop B with residues 268-272, and loop C with residues 327-343, which contain more hydrogen bonds than those in TtIPMDH. These regions in BcIPMDH differ in usage of determinants for thermostabilization from those in TtIPMDH.

For a full discussion, it is necessary to include a less thermostable protein. BsIPMDH, IPMDH from the mesophile *Bacillus subtilis*, is less thermostable than the moderately thermostable BcIPMDH (*6, 52*). The amino acid sequence of BsIPMDH is closer to that of BcIPMDH

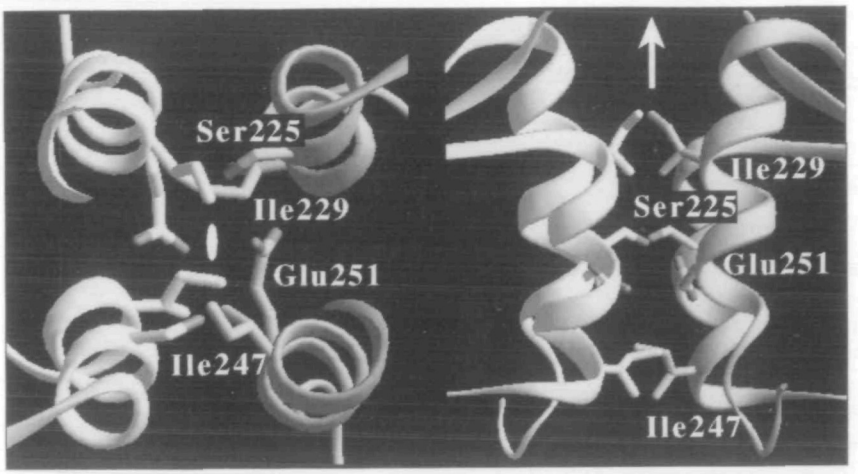

(a)

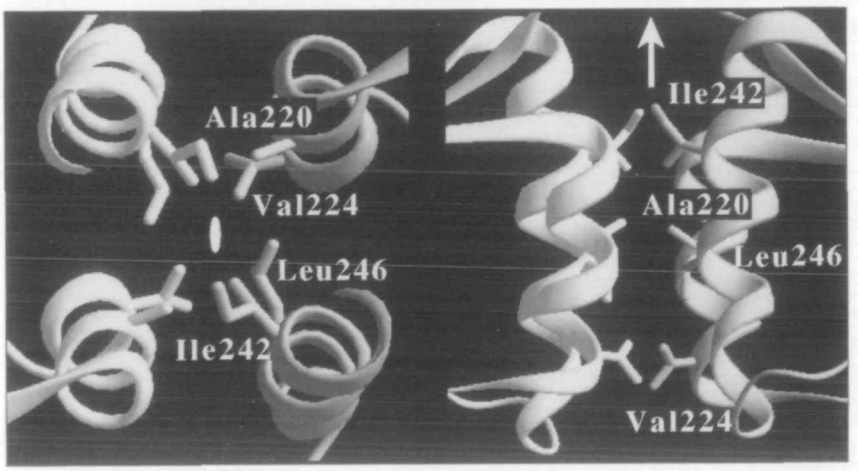

(b)

Fig. 7. **Four-helix-bundle structures in the subunit interfaces of BcIPMDH (a) and TtIPMDH (b).** Left is a view along the dyad axis of the dimer and its side view is on the right. The two subunits are drawn in different shades. Those of TtIPMDH are related by the crystallographic symmetry. These pictures were produced with the program RIBBONS (*22*).

TABLE IV. **Comparison of the structures in the terms of determinants for thermostabilization between BcIPMDH and TtIPMDH.**

Consistent change[a]	Inconsistent change[a]
Asp→Glu replacement	Increasing number of glycines
Increasing number of prolines	Decreasing number of hydrogen bonds
Increasing number of ion-pairs	Increasing volume of cavities
Stabilization of hydrophobic core	Decreasing capped helix termini

[a]With the proposed preference.

than to that of TtIPMDH (see Fig. 3). Moreover, BsIPMDH has the same number of residues as BcIPMDH, except for the loss of 3 residues in the C-terminal and insertion of 2 residues in loop A. Thus, it may be inferred that minor changes of primary structure occurred during adaptation to a slightly changed environment in BcIPMDH, while more drastic changes were involved for the higher thermostability of TtIPMDH. Although the three-dimensional structure of BsIPMDH has not yet been determined, it is possible to analyze the changes between BcIPMDH and BsIPMDH from a comparison of their sequences and the three-dimensional structure of BcIPMDH.

Loop B links the two adjacent β-strands which take part in forming a central β-sheet in the protein core. Since the region is distant from the active site, it may be possible to change the local structure with little effect on the enzymatic function. In fact, the structure around loop B of BcIPMDH [Fig. 8(b1)] is rather different from that of TtIPMDH [Fig. 8(b2)]. Arg268 in BcIPMDH forms a hydrogen bond with the carboxyl oxygen of Met99, which belongs to another loop (residues 98–102), and at the same time Arg268 forms a salt bridge with Asp270 within loop B (see also Fig. 1b for their electron densities). Lys173 also forms hydrogen bonds with two carbonyl oxygens of the loop. Since Lys173, Arg268, and Asp270 are not conserved in BsIPMDH (Fig. 3), similar hydrogen bonds can not be formed in BsIPMDH even though the length of the loop is the same as that of BcIPMDH. Although such solvent-exposed interactions are less effective for thermostabilization than buried ones (*1*), these hydrogen bonds and a salt bridge slightly increase the thermal resistance of BcIPMDH. In contrast, the corresponding loop of TtIPMDH contains distinct determinants for thermostabilization. Although in TtIPMDH there are two hydrogen bonds through Gln97 and one ion-pair between Asp98 and Arg264 [Fig. 8(b2)], they do not contribute greatly to the extreme thermostability because they are located on the molecular surface. Instead, loop B of TtIPMDH contains a gap of amino acid sequence (Fig. 3). Such shortening of the loop length is effective for thermostabilization of proteins (*7, 53–55*). Conversely, loop B of BcIPMDH is unnecessarily long to construct the framework

of the protein molecule. Moreover, Gly273 in BcIPMDH is replaced with a proline residue (Pro267). This replacement suggests that BcIPMDH contains surplus flexibility which may be removed with no effect on the function, as is also found at position 256 of BcIPMDH where the amino acid is the flexible threonine (Fig. 5b). These two changes could make TtIPMDH more resistant thermally. At loop B, with unnecessary length and surplus flexibility in the moderate thermophile, a salt bridge and hydrogen bonds exert enthalpic effects for stability. The extreme thermophile requires a drastic change of tertiary structure with high entropic effects. In addition, Gly263, which has glycine-specific dihedral angles ($\phi = 176°$, $\psi = -141°$), releases the strain of the main chain conformation caused by the drastic change required for the extreme thermostabilization.

The region around loop A [Fig. 8(a1)] also has more hydrogen bonds than the corresponding region of TtIPMDH [Fig. 8(a2)]. Arg148 of BcIPMDH forms two intersubunit salt bridges with Glu195′ and Glu202′ in the dimer (see also Fig. 1a for their electron densities). Asp158 is located near the N-terminus of the helix α_6 in the other subunit to form a capped structure. The aspartate residue also forms a hydrogen bond with Ser146. Other salt bridges are found between Glu195′ and Arg198′, and between Glu147 and Arg149 in each subunit. All these residues are conserved in both BcIPMDH and BsIPMDH, suggesting the presence of similar interactions in BsIPMDH. However, Glu147 and Arg149 in BcIPMDH are replaced with Lys147 and Tyr149, respectively, so that the salt bridge between the two residues is difficult to form in BsIPMDH. The salt bridge will contribute to the moderate thermostabilization as found in loop B. On the other hand, the region around loop A of TtIPMDH has only one salt bridge between Arg144 and Glu190′. Therefore, the region must contain distinct determinants. Loop A of BcIPMDH is longer than required to invert the chain direction, and protrudes into the solvent region without interactions with the rest of the protein. As might be expected, loop A of TtIPMDH is shortened by 3 residues (by 5 residues from BsIPMDH) to form a sharp, compact turn. However, little shortening of the length is observed from BsIPMDH to BcIPMDH, and, moreover, one proline residue (Pro151) is introduced in BcIPMDH. In the loop of BcIPMDH, there is a glycine residue (Gly152) with a left-handed-helical conformation of (ϕ, ψ) = (53, 24) to release torsional strain of the main-chain. Since loop A of TtIPMDH is sufficiently reduced, the protein does not require any other determinants, except for a salt bridge between Arg144 and Glu190′. On the other hand, for intermediate stabilization, BcIPMDH not only utilizes hydrogen bonds and salt bridges, but also in part mimics the usage of other determinants in loop B of TtIPMDH. Since this region is also distant from the active site, these changes should have little effect on the function. In the cases of EcIPMDH and StIPMDH which are less thermostable than TtIPMDH, the corresponding loop A is also longer than that of TtIPMDH and forms two additional hydrogen bonds absent in TtIPMDH (*7*).

The loop C region contains a new short β-sheet in BcIPMDH [Fig. 8(c1)], which is presumably important to stabilize this region. The corresponding loop of BsIPMDH has the same length. It would be interesting to know whether or not the loop has such a secondary structure in BsIPMDH, since the amino acid sequence is different (Fig. 3). By contrast, the corresponding loop C of TtIPMDH has no such β-sheet. Instead, TtIPMDH deletes 5 residues to make the loop less redundant [Figs. 3 and 8(c2)]. Furthermore, the conformation of this loop is extremely restricted by the three contiguous proline residues and the subsequent β-turn [Fig. 8(c2)]. Here it is important to note that Asp333 in the loop C region of BcIPMDH can be well superimposed on the corresponding residue of TtIPMDH, which participates in NAD binding (Fig. 5a). In order to stabilize the structure with no change in affinity for the cofactor, BcIPMDH forms a β-sheet through hydrogen bonds. TtIPMDH employs different strategies, deletion of unnecessary residues and replacement with proline residues, to reduce redundancy as an entropic effect. In addition, three glycine residues are introduced in the loop of TtIPMDH. One of them, Gly328, takes left-handed-helical dihedral angles of (ϕ, ψ) = (64, 81), to release conformational strain caused in the loop.

In the three loop regions, BcIPMDH and BsIPMDH seem to have some redundant parts with unnecessary lengths of amino acid sequence, but in BcIPMDH these are moderately stabilized by salt bridging and/or hydrogen bonding which are brought about by replacement with appropriate amino acids. As residues on the molecular surface have little role in the stability (*1*), it is reasonable to consider that such hydrogen bonding is an appropriate determinant for moderate thermostabilization. On the other hand, TtIPMDH does not contain such unnecessary residues. Furthermore, all proline residues are utilized to restrict the main-chain conformations in loop regions. These prolines play an important role in the extreme thermostabilization by reducing surplus flexibility without altering the enzymatic function. Such "unnecessary" regions can be regarded as "structural redundancy" in protein structure. The difference in usage of determinants at such redundant parts suggests two distinct strategies for thermostabilization in the two different organisms, *B. coagulans* and *T. thermophilus*. For moderate thermostabilization, the region with some structural redundancy is reinforced by salt bridges and/or hydrogen bonds whereas such redundancy is reduced without reinforcement for extreme thermostabilization. Similar reduction is, in part, applied for the thermostabilization of BcIPMDH. Prolines are extensively used in both the moderate and the extreme thermophilic proteins. A direct correlation between the number of prolines and thermostability (15 in BsIPMDH, 18 in BcIPMDH and 25 in TtIPMDH) is in agreement with other observations (*56, 57*). In addition, when drastic changes of loop conformation occur due to the extreme thermostabilization, some glycines are effectively utilized to release strains caused on the backbone. This is presumably one of the reasons why TtIPMDH has more glycines than BcIPMDH. The increase of hydrogen bonds in BcIPMDH is thus consistent with the moderate thermostabilization. The other determinants which seem to be inconsistent with those of TtIPMDH (Table IV) can be ascribed to such hydrogen bondings and result in additional advantages for BcIPMDH.

Another example in which a highly thermostable protein uses a less-redundant structure rather than a structure reinforced by hydrogen bonds is as follows. Kelly *et al.* indicated some determinants for thermostabilization in

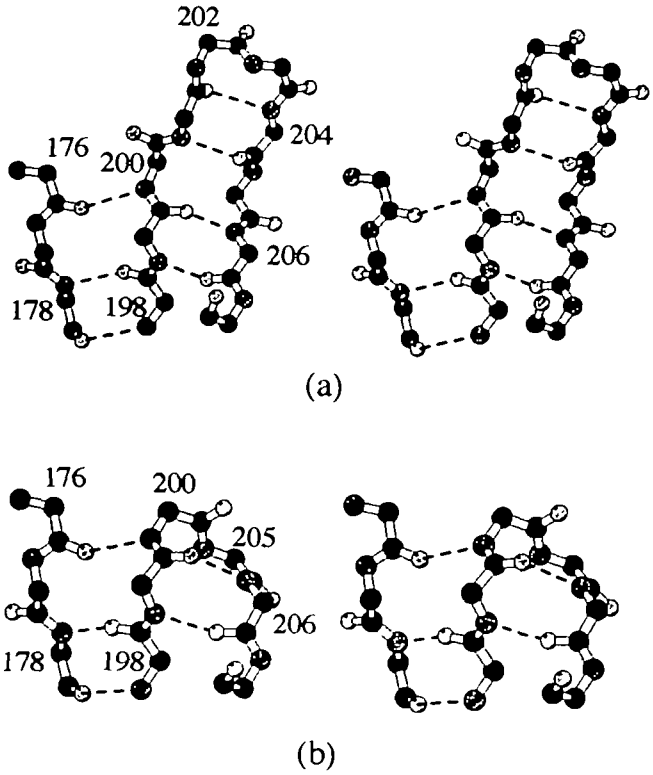

Fig. 9. **Stereo-pair diagrams of local structures (residues 176-178 and 198-207) of cMDH (a) and tMDH (b).** The broken lines indicate hydrogen bonds. The corresponding residues, 201-204 in cMDH are missing in tMDH. The side chains are suppressed for clarification. The diagrams were produced with the program MOLSCRIPT (*27*).

malate dehydrogenase of *Thermus flavus* (tMDH) (*37*) by comparing its structure with that of the cytoplasmic enzyme of porcine heart (cMDH) (*58*). We inspected the two structures with their coordinates ("4MDH" for cMDH and "1BMD" for tMDH in PDB). The region of residues 198-207 in cMDH has a β-sheet with two anti-parallel strands linked by a β-turn (Fig. 9a). For an adaptation to higher temperatures, it seems possible to remove the 4 residues around the turn because they are distant from the active site and protrude into the solvent region. In fact, in tMDH, which is more thermostable than cMDH, these residues are removed even though this occurs in a region of well-defined secondary structure (Fig. 9b).

CONCLUSION

The present analysis of moderately thermophilic BcIPMDH has made it possible to compare the structure with extremely thermophilic TtIPMDH. Some apparently inconsistent changes found in BcIPMDH reveal a difference in usage of thermostabilization determinants between the two proteins. Although many more enzymes would have to be studied to reach a general conclusion, the present comparison leads us to the following conclusion for the present cases. For moderate thermostabilization, the tertiary structure is reinforced through salt bridges and hydrogen bonds, which are made possible by replacement with appropriate amino acids. When it is no longer possible to adapt to an extremely high temperature by such replacements, a drastic change of the tertiary structure is required, in which structural redundancies are reduced for extreme thermostabilization. When strains arise in the backbone, glycine residues are introduced to release them. Thus, there seem to be at least two strategies for thermostabilization in nature. One is "reinforcement of structure" with enthalpic effects which results in minor changes of thermostabilization. The other is "reduction of structural redundancy," which causes entropic reduction of unfolded proteins and is required when the former strategy is insufficient to stabilize the structure at higher temperature. This proposal should be confirmed by analyses of several other enzymes.

The two strategies are applicable to designing moderately or extremely thermostable proteins. Most of the redundant parts are located in loop regions. There are two types of loops in general. One connects two secondary structures. Such a loop can be a target for adjusting protein thermostability. However, it should be noted that a long insertion of amino acids makes the situation more complicated. The second type of loop is concerned with function. In such a loop, it is difficult to reduce the structural redundancy, but it may be possible, as found in loop C and at the Thr256 replaced with Pro in TtIPMDH. For practical application, a database of known structures used in crystallographic model building (*16*) may facilitate the design of thermostabilized protein structures.

We are grateful to N. Sakabe and N. Watanabe for facilities and help during data collection at the Photon Factory (Tsukuba). We thank R.J. Poljak and J.N. Jansonius for helpful discussions and comments on the manuscript.

REFERENCES

1. Matthews, B.W. (1991) Mutational analysis of protein stability. *Curr. Opin. Struct. Biol.* **1**, 17-21
2. Fersht, A.R. and Serrano, L. (1993) Principles of protein stability derived from protein engineering experiments. *Curr. Opin. Struct. Biol.* **3**, 75-83
3. Quinol, E., Perez-Pons, J.A., and Mozo-Villarias, A. (1996) Analysis of protein conformational characteristics related to thermostability. *Protein Eng.* **9**, 265-271
4. Stieglitz, B.I. and Calvo, J.M. (1974) Distribution of the isopropylmalate pathway to leucine among diverse bacteria. *J. Bacteriol.* **118**, 935-941
5. Sharp, R.J., Bown, K.J., and Atkinson, A. (1980) Phenotypic and genotypic characterization of some thermophilic species of *Bacillus*. *J. Gen. Microbiol.* **117**, 201-210
6. Sekiguchi, T., Harada, Y., Shishido, K., and Nosoh, Y. (1984) Cloning of β-isopropylmalate dehydrogenase from *Bacillus coagulans* in *Escherichia coli* and purification and properties of the enzyme. *Biochim. Biophys. Acta* **788**, 267-273
7. Wallon, G., Kryger, G., Lovett, S.T., Oshima, T., Ringe, D., and Petsko, G.A. (1997) Crystal structure of *Escherichia coli* and *Salmonella typhimurium* 3-isopropylmalate dehydrogenase and comparison with their thermophilic counterpart from *Thermus thermophilus*. *J. Mol. Biol.* **266**, 1016-1031
8. Tsuchiya, D., Matsumoto, O., Gorai, T., Sekiguchi, T., Nosoh, Y., and Takenaka, A. (1996) Crystallization and preliminary x-ray analysis of 3-isopropylmalate dehydrogenase from the moderate facultative thermophile, *Bacillus coagulans*. *Acta Cryst.* **D52**, 1030-1032
9. Sakabe, N. (1991) X-ray diffraction data collection system for modern protein crystallography with a weissenberg camera and an imaging plate using synchrotron radiation. *Nucl. Instrum. Methods* **A303**, 448-463

10. Higashi, T. (1989) The processing of diffraction data taken on a screenless weissenberg camera for macromolecular crystallography. *J. Appl. Cryst.* **22**, 9-18
11. Collaborative Computational Project, Number 4 (1994) The CCP4 suite: programs for protein crystallography. *Acta Cryst.* **D50**, 760-763
12. Imada, K., Sato, M., Tanaka, N., Katsube, Y., Matsuura, Y., and Oshima, T. (1991) Three-dimensional structure of a highly thermostable enzyme, 3-isopropylmalate dehydrogenase of *Thermus thermophilus* at 2.2 Å resolution. *J. Mol. Biol.* **222**, 725-738
13. Navaza, J. (1994) AMoRe: an automated package for molecular replacement. *Acta Cryst.* **A50**, 157-163
14. Tsuchiya, D. and Takenaka, A. (1998) R_{omit} profile analysis for molecular replacements. *Acta Cryst.* **D54**, in press
15. Zhang, K.Y.J. (1993) *SQUASH*—Combining constraints for macromolecular phase refinement and extension. *Acta Cryst.* **D49**, 213-222
16. Jones, T.A., Zou, J.Y., Cowan, S.W., and Kjeldgaard, M. (1991) Improved methods for building protein models in electron density maps and the location of errors in these models. *Acta Cryst.* **A47**, 110-119
17. Brünger, A.T. (1992) *X-PLOR. Version 3.1. A System for X-Ray Crystallography and NMR.* Yale University Press, New Haven, CT
18. Brünger, A.T. (1992) Free-R value: a novel statistical quantity for assessing the accuracy of crystal structures. *Nature* **355**, 472-475
19. Morris, A.L., MacArthur, M.W., Hutchinson, E.G., and Thornton, J.M. (1992) Stereochemical quality of protein structure coordinates. *Proteins* **12**, 345-364
20. Sekiguchi, T., Ortega-Cesena, J., Nosoh, Y., Ohashi, S., Tsuda, K., and Kanaya, S. (1986) DNA and amino-acid sequences of 3-isopropylmalate dehydrogenase of *Bacillus coagulans*. Comparison with the enzymes of *Saccharomyces cerevisiae* and *Thermus thermophilus*. *Biochim. Biophys. Acta* **867**, 36-44
21. Luzzati, P.V. (1952) Traitement statistique des erreurs dans la determination des structures cristallines. *Acta Cryst.* **5**, 802-810
22. Carson, M. (1991) Ribbons 2.0. *J. Appl. Cryst.* **24**, 958-961
23. Kagawa, Y., Nojima, H., Nukiwa, N., Ishizuka, M., Nakajima, T., Yasuhara, T., Tanaka, T., and Oshima, T. (1984) High guanine plus cytosine content in third letter of codons of an extreme thermophile. *J. Biol. Chem.* **259**, 2956-2960
24. Imai, R., Sekiguchi, T., Nosoh, Y., and Tsuda, K. (1987) The nucleotide sequence of 3-isopropylmalate dehydrogenase gene from *Bacillus subtilis*. *Nucleic Acids Res.* **15**, 4988
25. Hurley, J.H. and Dean, A.M. (1994) Structure of 3-isopropylmalate dehydrogenase in complex with NAD^+: ligand-induced loop closing and mechanism for cofactor specificity. *Structure* **2**, 1007-1016
26. Kadono, S., Sakurai, M., Moriyama, H., Sato, M., Hayashi, Y., Oshima, T., and Tanaka, N. (1995) Ligand-induced changes in the conformation of 3-isopropylmalate dehydrogenase from *Thermus thermophilus*. *J. Biochem.* **118**, 745-752
27. Kraulis, P.J. (1991) MOLSCRIPT: A program to produce both detailed and schematic plots of protein structures. *J. Appl. Cryst.* **24**, 946-950
28. Matthews, B.W., Nicholson, H., and Becktel, W.J. (1987) Enhanced protein thermostability from site-directed mutations that decrease the entropy of unfolding. *Proc. Natl. Acad. Sci. USA* **84**, 6663-6667
29. Yutani, K., Hayashi, S., Sugisaki, Y., and Ogasahara, K. (1991) Role of conserved proline residues in stabilizing tryptophan synthase α subunit: analysis by mutants with alanine or glycine. *Proteins* **9**, 90-98
30. Watanabe, K., Masuda, T., Ohashi, H., Mihara, H., and Suzuki, Y. (1994) Multiple proline substitutions cumulatively thermostabilize *Bacillus cereus* ATCC7064 oligo-1,6-glucosidase. *Eur. J. Biochem.* **226**, 277-283
31. Argos, P., Rossmann, M.G., Grau, U.M., Zuber, H., Frank, G., and Tratschin, J.D. (1979) Thermal stability and protein structure. *Biochemistry* **18**, 5698-5703
32. Ishikawa, K., Kimura, S., Kanaya, S., Morikawa, K., and Nakamura, H. (1993) Structural study of mutants of *Escherichia coli* ribonuclease HI with enhanced thermostability. *Protein Eng.* **6**, 85-91
33. Amaki, Y., Nakano, H., and Yamane, T. (1994) Role of cysteine residues in esterase from *Bacillus stearothermophilus* and increasing its thermostability by the replacement of cysteines. *Appl. Microbiol. Biotechnol.* **40**, 664-668
34. Perutz, M.F. (1978) Electrostatic effects in proteins. *Science* **201**, 1187-1191
35. Hennig, M., Darimont, B., Sterner, R., Kirschner, K., and Jansonius, J.N. (1995) 2.0 Å structure of indole-3-glycerol phosphate synthase from the hyperthermophile *Sulfolobus solfataricus*: possible determinants of protein stability. *Structure* **3**, 1295-1306
36. Yip, K.S.P., Stillman, T.J., Britton, K.L., Artymiuk, P.J., Baker, P.J., Sedelnikova, S.E., Engel, P.C., Pasquo, A., Chiaraluce, R., Consalvi, V., Scandurra, R., and Rice, D.W. (1995) The structure of *Pyrococcus furiosus* glutamate dehydrogenase reveals a key role for ion-pair networks maintaining enzyme stability at extreme temperatures. *Structure* **3**, 1147-1158
37. Kelly, C.A., Nishiyama, M., Ohnishi, Y., Beppu, T., and Birktoft, J. (1993) Determinants of protein thermostability observed in the 1.9-Å crystal structure of malate dehydrogenase from thermophilic bacterium *Thermus flavus*. *Biochemistry* **32**, 3913-3922
38. Tanner, J.N., Hecht, R.M., and Krause, K.L. (1996) Determinants of enzyme thermostability observed in the molecular structure of *Thermus aquaticus* D-glyceraldehyde-3-phosphate dehydrogenase at 2.5 Å resolution. *Biochemistry* **35**, 2597-2609
39. Miller, S., Janin, J., Lesk, A.M., and Chothia, C. (1987) Interior and surface of monomeric proteins. *J. Mol. Biol.* **196**, 641-656
40. Dao-pin, S., Sauer, U., Nicholson, H., and Matthews, B.W. (1991) Contributions of engineered surface salt bridges to the stability of T4 lysozyme determined by directed mutagenesis. *Biochemistry* **30**, 7142-7153
41. Baker, E.N. and Hubbard, R.E. (1984) Hydrogen bonding in globular proteins. *Prog. Biophys. Mol. Biol.* **44**, 97-179
42. Serrano, L. and Fersht, A.R. (1989) Capping and α-helix stability. *Nature* **342**, 296-299
43. Nicholson, H., Becktel, W.J., and Matthews, B.W. (1988) Enhanced protein thermostability from designed mutations that interact with α-helix dipoles. *Nature* **336**, 651-656
44. Horovitz, A., Matthews, J.M., and Fersht, A.R. (1992) α-Helix stability in proteins: II. Factors that influence stability at an internal position. *J. Mol. Biol.* **227**, 560-568
45. O'Neil, K.T. and DeGrado, W.F. (1990) A thermodynamic scale for the helix-forming tendencies of the commonly occurring amino acids. *Science* **250**, 646-651
46. Yutani, K., Ogasahara, K., Tsujita, T., and Sugino, Y. (1987) Dependence of conformational stability on hydrophobicity of the amino acid residue in a series of variant proteins substituted at a unique position of tryptophan synthase α subunit. *Proc. Natl. Acad. Sci. USA* **84**, 4441-4444
47. Blaber, M., Lindstrom, J.D., Gassner, N., Xu, J., Heinz, D.W., and Matthews, B.W. (1993) Energetic cost and structural consequences of burying a hydroxyl group within the core of a protein determined from Ala→Ser and Val→Thr substitutions in T4 lysozyme. *Biochemistry* **32**, 11363-11373
48. Kellis, J.T., Jr., Nyberg, K., Sali, D., and Fersht, A.R. (1988) Contribution of hydrophobic interactions to protein stability. *Nature* **333**, 784-786
49. Kirino, H., Aoki, M., Aoshima, M., Hayashi, Y., Ohba, M., Yamagishi, A., Wakagi, T., and Oshima, T. (1994) Hydrophobic interaction at the subunit interface contributes to the thermostability of 3-isopropylmalate dehydrogenase from an extreme thermophile, *Thermus thermophilus*. *Eur. J. Biochem.* **220**, 275-281
50. Kleywegt, G.J. and Jones, T.A. (1994) Detection, delineation, measurement and display of cavities in macromolecular structures. *Acta Cryst.* **D50**, 178-185
51. Chan, M.K., Mukund, S., Kletzin, A., Adams, M.W.W., and

Rees, D.C. (1995) Structure of a hyperthermophilic tungstopterin enzyme, aldehyde ferredoxin oxidoreductase. *Science* **267**, 1463-1469
52. Numata, K., Muro, M., Akutsu, N., Nosoh, Y., Yamagishi, A., and Oshima, T. (1995) Thermal stability of chimeric isopropylmalate dehydrogenase genes constructed from a thermophile and a mesophile. *Protein Eng.* **8**, 39-45
53. Russell, R.J.M., Hough, D.W., Danson, M.J., and Taylor, G.L. (1994) The crystal structure of citrate synthase from the thermophilic archaeon, *Thermoplasma acidophilum*. *Structure* **2**, 1157-1167
54. Macedo-Ribeiro, S., Darimont, B., Sterner, R., and Huber, R. (1996) Small structural changes account for the high thermostability of 1[4Fe-4S] ferredoxin from the hyperthermophilic bacterium *Thermotoga maritina*. *Structure* **4**, 1291-1301
55. Knegtel, R.M.A., Wind, R.D., Rozeboom, H.J., Kalk, K.H., Buitelaar, R.M., Dijkhuizen, L., and Dijkstra, B.W. (1996) Crystal structure at 2.3 Å resolution and revised nucleotide sequence of the thermostable cyclodextrin glycosyltransferase from *Thermoanaerobacterium thermosulfurigenes* EM1. *J. Mol. Biol.* **256**, 611-622
56. Suzuki, Y., Oishi, K., Nakano, H., and Nagayama, T. (1987) A strong correlation between the increase in number of proline residues and the rise in thermostability of five *Bacillus* oligo-1,6-glucosidases. *Appl. Microbiol. Biotechnol.* **26**, 546-551
57. Nakao, M., Nakayama, T., Kakudo, A., Inohara, M., Harada, M., Omura, F., and Shibano, Y. (1994) Structure and expression of a gene coding for thermostable α-glucosidase with a broad substrate specificity from *Bacillus* sp. SAM1606. *Eur. J. Biochem.* **220**, 293-300
58. Birktoft, J.J., Rhodes, G., and Banaszak, L.J. (1989) Refined crystal structure of cytoplasmic malate dehydrogenase at 2.5-Å resolution. *Biochemistry* **28**, 6065-6081